Image Similarity Measurement by an Integrated Probabilistic Histogram

Tatsuyuki Kawamura Takahiro Ueoka Yutaka Kiuchi
Yasuyuki Kono Masatsugu Kidode

{tatsu-k,taka-ue,yutaka-k,kono,kidode}@is.aist-nara.ac.jp
Graduate School of Information Science, Nara Institute of Science and Technology
8916-5 Takayama, Ikoma, Nara 630-0192, Japan

Abstract

In this paper, we present a useful histogram in order to reduce sensor noise effect and get to similar measures. This histogram is constructed in HSV color space using the probabilistic representation of color distribution. To prove the effectiveness of the approach, we conducted two experiments in comparison with the conventional one.

1 Introduction

Object recognition from color images has been widely tackled recently. In order to discriminate similar objects, a color histogram is often employed [1, 2, 3], e.g, a hue color histogram. However, an image captured by a camera certainly contains additional sensor noise. Using a conventional histogram, the afore-mentioned noise reduces the object recognition rate.

In this paper, we propose a novel probabilistic histogram, named an Integrated Probabilistic Histogram (IPH), which enables effective object recognition called . The IPH employs a probabilistic representation of color distribution in HSV color space. The IPH is made from hue data using the probabilistic behaviors of saturation and value data. The IPH is represented by the summed densities of probabilistic distributions. The IPH also has the advantage of representing a certain density if the image shows achromatic color. We conducted two experiments to evaluate our IPH; the results show its effectiveness in recognizing objects.

2 Noise Model

The image data captured by a camera contains additional sensor noise. The noise model is shown in equation (1). u_{est} and σ_u are respectively the standard deviation and the estimated value.

$$\hat{u} = u_{est} \pm \sigma_u. \tag{1}$$

In this paper, we define red, green, and blue values as $R, G, andB$, and also represent individual sensor noises of RGB colors, σ_R, σ_G, and σ_B in RGB space.

A standard deviation of a certain function $q(u, \ldots, w)$ is calculated by equation (2).

$$\sigma_q = \sqrt{\left(\frac{\partial q}{\partial u}\sigma_u\right)^2 + \ldots + \left(\frac{\partial q}{\partial w}\sigma_w\right)^2}. \tag{2}$$

Note that $\sigma_u, \ldots, \sigma_w$ are supposed by captured images. The predicted uncertainty σ_q can be computed if $\sigma_u, \ldots, \sigma_w$ are independent, random and relatively small [4]. $\partial q/\partial u$ and $\partial q/\partial w$ represent the partial derivatives of q in $u, \ldots, w$.

In this paper, we define a shape of sensor noise as the following kernel:

$$K(x) = \frac{1}{\sqrt{2\pi}\sigma} e^{-\frac{(x-u)^2}{2\sigma^2}}. \tag{3}$$

In order to employ the kernel, we agreed on Gevers's kernel because photons fit well into Gaussian distribution when the average number of the counts of photons is large [5].

3 RGB-HSV Conversion

Values of H, S, V (and Z) in HSV color space are given by R, G, and B in RGB color space by equation (4) $\sim$ (7). In this paper, R, G, and B are limited to $0 \leq R, G, B < \alpha$. H is also limited to $0° \leq H < \beta°$. The range of S and V are $0 \leq S, V < \alpha$.

Equation (4) gives the value of V.

$$V = max(R, G, B). \tag{4}$$

The minimum value of Z in R, G, and B values is given by the following equation:

$$Z = min(R, G, B). \tag{5}$$

Saturation value S is transformed by equation (6).

$$S = \alpha\left(\frac{V - Z}{V}\right). \tag{6}$$

H is given by equation (7). Suppose that $X \equiv V$

means that X $(X \in R, G, B)$ corresponds with V.

$$H = \begin{cases} \beta\left(\dfrac{G-B}{V-Z}\right), & R \equiv V \\ \beta\left(2+\dfrac{B-R}{V-Z}\right), & G \equiv V \\ \beta\left(4+\dfrac{R-G}{V-Z}\right). & B \equiv V \end{cases} \quad (7)$$

4 The Integrated Probabilistic Histogram

The aim of the study is to be able to represent the probabilistic behavior of sensor noise on a hue color histogram. In order to realize such a representation, a calculation of standard deviation in HSV color space is required. The average and standard deviation of both V and Z, however, cannot be calculated using differentiation because of the functions of max and min.

A certain probability of $p_y(x)$ in the Gaussian distribution $y \in R, G, B$ leads to equation (3).

$$p_y(x) = K^y(x) = \frac{1}{\sqrt{2\pi}\sigma_y} e^{-\frac{(x-u_y)^2}{2\sigma_y^2}} \quad (8)$$

Maximum probability $P_{X_V}(x)$ $(X \in R, G, B)$ in RGB color space is given by:

$$\begin{aligned} P_{R_V}(x) &= p_R(x)\int_{-\infty}^{x}\int_{-\infty}^{u} p_G(u)p_B(v)dvdu \\ P_{G_V}(x) &= p_G(x)\int_{-\infty}^{x}\int_{-\infty}^{u} p_B(u)p_R(v)dvdu \\ P_{B_V}(x) &= p_B(x)\int_{-\infty}^{x}\int_{-\infty}^{u} p_R(u)p_G(v)dvdu \end{aligned} \quad (9)$$

Equation (9) gives probability V in x as

$$\begin{aligned} P_V(x) = {} & P_{R_V}(x)(1-P_{G_V}(x))(1-P_{B_V}(x)) \\ & +(1-P_{R_V}(x))P_{G_V}(x)(1-P_{B_V}(x)) \\ & +(1-P_{R_V}(x))(1-P_{G_V}(x))P_{B_V}(x). \end{aligned} \quad (10)$$

Equation (10) gives an average of V as

$$u_V = \frac{\int_{-\infty}^{\infty} xP_V(x)dx}{\int_{-\infty}^{\infty} P_V(x)dx} \quad (11)$$

Finally, a standard deviation of V is computed by:

$$\sigma_V = \int_{-\infty}^{\infty} P_V(x)(x-u_V)^2 dx \quad (12)$$

The average and standard deviation of Z are also given by (5). Maximum probability $P_{X_Z}(x)$ $(X \in R, G, B)$ in RGB color space is given by:

$$\begin{aligned} P_{R_Z}(x) &= p_R(x)\int_{x}^{\infty}\int_{u}^{\infty} p_G(u)p_B(v)dvdu \\ P_{G_Z}(x) &= p_G(x)\int_{x}^{\infty}\int_{u}^{\infty} p_B(u)p_R(v)dvdu \\ P_{B_Z}(x) &= p_B(x)\int_{x}^{\infty}\int_{u}^{\infty} p_R(u)p_G(v)dvdu \end{aligned} \quad (13)$$

Equation (13) gives probability Z in x as

$$\begin{aligned} P_Z(x) = {} & P_{R_Z}(x)(1-P_{G_Z}(x))(1-P_{B_Z}(x)) \\ & +(1-P_{R_Z}(x))P_{G_Z}(x)(1-P_{B_Z}(x)) \\ & +(1-P_{R_Z}(x))(1-P_{G_Z}(x))P_{B_Z}(x). \end{aligned} \quad (14)$$

Equation (14) gives an average of Z as

$$u_Z = \frac{\int_{-\infty}^{\infty} xP_Z(x)dx}{\int_{-\infty}^{\infty} P_Z(x)dx}. \quad (15)$$

Finally, a standard deviation of Z is computed by:

$$\sigma_Z = \int_{-\infty}^{\infty} P_Z(x)(x-u_Z)^2 dx. \quad (16)$$

Substitution of (6) in (2) gives the standard deviation of S as

$$\sigma_S = \alpha\sqrt{\frac{Z^2\sigma_V^2 + V^2\sigma_Z^2}{V^4}}. \quad (17)$$

Substitution of (7) in (2) gives the standard deviation of H as

$$\sigma_H = \begin{cases} \sigma_{RGB}(G,B), & R \equiv V \\ \sigma_{RGB}(B,R), & G \equiv V \\ \sigma_{RGB}(R,G). & B \equiv V \end{cases} \quad (18)$$

where $\sigma_{RGB}(x,y)$ in (18) is given by:

$$\begin{aligned} \sigma_{RGB}(x,y) = {} & \alpha\beta\sqrt{\frac{(x-y)^2(V^2\sigma_S^2 + S^2\sigma_V^2)}{V^4S^4}} \\ & \sqrt{\frac{+S^2V^2(\sigma_x^2+\sigma_y^2)}{V^4S^4}}. \end{aligned} \quad (19)$$

Finally, the probabilistic behavior of sensor noise can be computed on a hue color histogram by the equations (12), (17), and (18) in HSV color space and (16). The probabilistic hue histogram is given

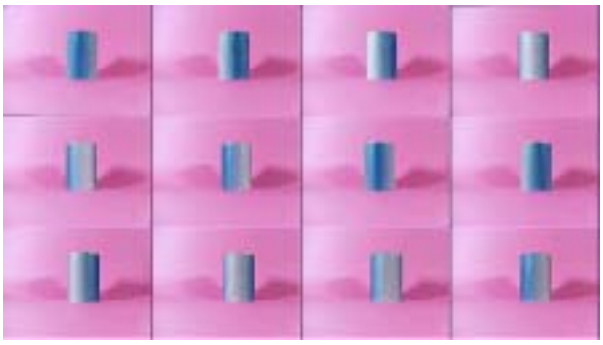

Figure 1: A cylinder target changing satulation and value along with the circumferential (Top : 0°, 30°, 60°, 90°. Middle : 120°, 150°, 180°, 210°, Bottom : 240°, 270°, 300°, 330°.)

by equation (20). The histogram also has the ability of computing achromatic color in the histogram.

$$\hat{f}_H(t) = \frac{1}{n}\sum_{i=1}^{n}\int_{h(t-1)}^{ht} K_i^H(x)dx. \ \{t|t = 1, 2, \ldots, \frac{\beta}{h}\} \quad (20)$$

where n is the amount of image pixels that are selected to make the histogram, t is the parameter of bin in the histogram, and h is the width of bin.

5 Experiments

We conducted two experiments to evaluate the quality of the IPH. In the experiment, the IPH was compared with a conventional/simple hue histogram. Note that parameters α and β were set as $\alpha = 255$, and $\beta = 359$. R, G, B, H, S, V, and Z were over 1 interval. The experiments were conducted on a cylindrical target having a gradual circumferential pattern change of saturation and value. The difference between the source histogram and a target histogram was computed using the Sum of Absolute Differences (SAD) in each histogram. The conditions of the experiments are shown as follows:

C1: A comparison between the same posture images

C2: A comparison between different posture images

5.1 Methods

Cam1
TYPE : SONY Entertainment Vision Sensor (EVIS) [6]
SD : $\sigma_R = 1.01,\ \sigma_G = 0.86,\ \sigma_B = 1.04$

Cam2
TYPE : ELMO UN43H (ObjectCam) [3]
SD : $\sigma_R = 3.52,\ \sigma_G = 2.23,\ \sigma_B = 3.20$

Cam3
TYPE : I-O DATA USB-CCD
SD : $\sigma_R = 4.19,\ \sigma_G = 2.35,\ \sigma_B = 3.41$

Figure 1 depicts 12 postures of the cylindrical target. 10 images were continuously captured in each posture over 30° intervals. The evaluated cameras all got 120 images in the same environment condition.

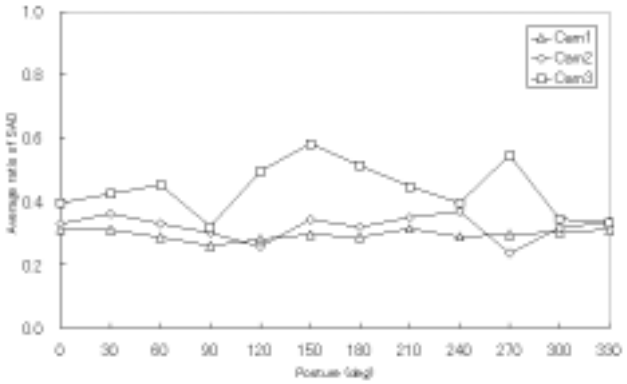

Figure 2: Average ratio of SAD between the same postures

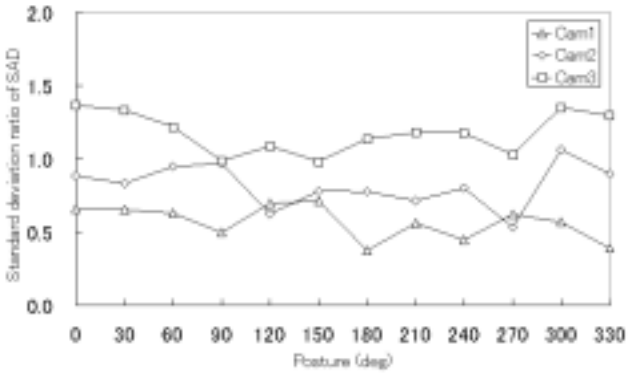

Figure 3: Standard deviation ratio of SAD between the same postures

5.2 Results

Figure 2 shows the average SAD ratio of the IPH on the conventional hue histogram in condition C1. The vertical axis represents an evaluated value where the average error of SAD on the IPH was divided by the average error of SAD on the conventional histogram. In the *Cam1* and *Cam2* condition, each total average error showed less than 0.4 points. In all camera conditions, the total summed average errors were 0.30 in *Cam1*, 0.32 in *Cam2*, and 0.44 in *Cam3*.

Figure 3 illustrates the standard deviation SAD ratio on the IPH to the conventional hue histogram in condition C1. The vertical axis represents an evaluated value as the standard deviation error of SAD on the IPH, which was divided by the standard deviation error of SAD on the conventional histogram. In all camera conditions, the total summed standard deviation errors were 0.57 in *Cam1*, 0.81 in *Cam2*, and 1.18 in *Cam3*.

Figure 4 describes the average SAD ratio on the IPH to the conventional hue histogram in condition C2. The source posture was set at 0° posture. The vertical axis represents an evaluated value where the average error of SAD on the IPH was divided by the

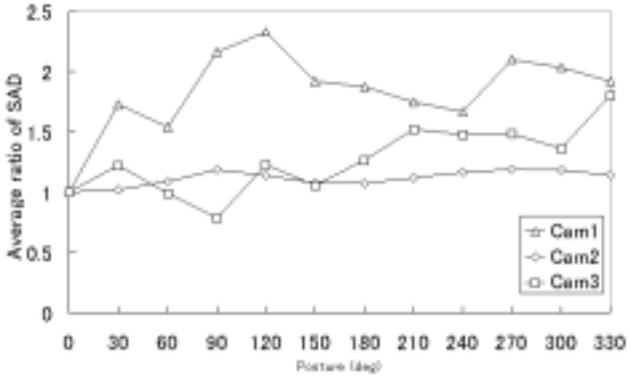

Figure 4: Average ratio of SAD between different postures

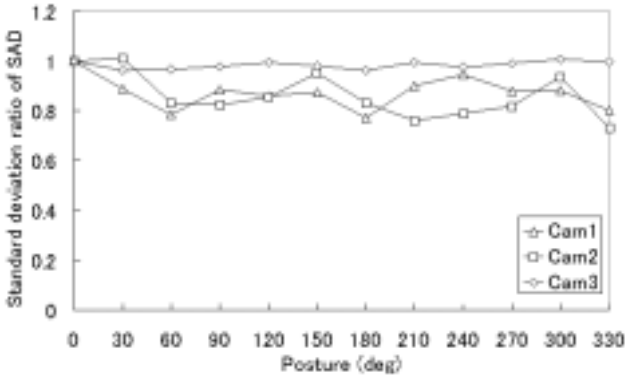

Figure 5: Standard deviation ratio of SAD between different postures

average error of SAD on the conventional histogram. In all camera conditions, the total summed average errors were 1.90 in *Cam1*, 1.13 in *Cam2*, and 1.29 in *Cam3*.

Figure 5 depicts the standard deviation SAD ratio on the IPH to the conventional hue histogram in condition C1. The source posture was set at 0° posture. The vertical axis represents an evaluated value where the standard deviation error of SAD on the IPH was divided by a standard deviation error of SAD of the conventional histogram. In all camera conditions, the total summed standard deviation errors were 0.86 in *Cam1*, 0.98 in *Cam2*, and 0.84 in *Cam3*.

5.3 Discussions

In condition C1, the total summed average errors were 0.30 in *Cam1*, 0.32 in *Cam2*, and 0.44 in *Cam3*. The results show that the IPH depresses the average error of SAD among the same posture images less than in the conventional histogram. In the C2 condition of the experiments, the total summed average errors were 1.90 in *Cam1*, 1.13 in *Cam2*, and 1.29 in *Cam3*. The two results show the effective suppression of the average error of SAD among the different posture images. These contrasting results between C1 and C2 give us considerable benefit in discriminating objects on a vision-based application.

The results of the C1 condition experiment are 0.57 in *Cam1*, 0.81 in *Cam2*, and 1.18 in *Cam3* in the standard deviation SAD ratio of the IPH to the conventional histogram. Also, the results of the C2 are 0.86 in *Cam1*, 0.98 in *Cam2*, and 0.84 in *Cam3*. In those results, depressions of standard deviation are shown, except for *Cam3*. The results show that the IPH provides the system with stability for object recognition.

We believe that the proposed method enables a vision-based system to be able to identify an object precisely and stably on the HSV color space.

6 Concluding Remarks

In this paper, we proposed the Integrated Probabilistic Histogram (IPH) to suppress sensor noise caused by a camera device. The experimental results show that the IPH is higher in 1) the discrimination ability for detecting similar images and 2) the stability of object detection than in the conventional hue histogram. The future work of this study is to minimize a comparison error between approximately the same images and to stabilize the error using a novel near modeling of sensor noise for high-speed image processing.

Acknowledgement

This research is supported by Core Research for Evolutional Science and Technology (CREST) Program "Advanced Media Technology for Everyday Living" of Japan Science and Technology Agency (JST).

References

[1] T. Gevers and W.M. Smeulders, "Color Based Object Recognition," *Pattern Recognition*, 32, pp.453–464, 1999.

[2] S. Sural, G. Qian and S. Pramaic, "A Histogram with Perceptually Smooth Color Transition for Image Retrieval," *Proc. 4th International Conference on Computer Vision, Pattern Recognition and Image Processing*, pp.664–667, 2002.

[3] T. Ueoka, T. Kawamura, Y. Kono and M. Kidode, "I'm Here!: a Wearable Object Remembrance Support System," *Proc. 5th International Symposium on Human Computer Interaction with Mobile Devices and Services*, pp.422–427, 2003.

[4] J.R. Taylor, "An Introduction to Error Analysis," *University Science Books*, 1982.

[5] T. Gevers, "Robust Histogram Construction from Color Invariants," *Proc. 8th International Conference on Computer Vision*, pp.615–621, 2001.

[6] T. Sugiyama, S. Yoshimura, R. Suzuki and H. Sumi, "A 1/4-inch QVGA Color Imaging and 3-D Sensing CMOS Sensor with Analog Frame Memory," *Proc. IEEE International Solid-State Circuit Conference*, pp.434–435 and 479, 2002.